

# Study of Two-photon Lithography using Optical Diffraction Tomography

Qi Shao<sup>1</sup>, Yanping He<sup>2</sup>, Renjie Zhou<sup>2, #</sup> and Shih-chi Chen<sup>1, #</sup>

<sup>1</sup> Department of Mechanical and Automation Engineering, The Chinese University of Hong Kong, Shatin, New Territories, Hong Kong, China

<sup>2</sup> Department of Biomedical Engineering, The Chinese University of Hong Kong, Shatin, New Territories, Hong Kong SAR, China

# Corresponding Author / Email: [rjzhou@cuhk.edu.hk](mailto:rjzhou@cuhk.edu.hk); [sochen@mae.cuhk.edu.hk](mailto:sochen@mae.cuhk.edu.hk)

KEYWORDS: 3D printing, two-photon polymerization, high-speed characterization, optical diffraction tomography

---

*Two-photon photopolymerization (TPP) has recently become a popular method for fabricating 3D micro- and nanostructures. However, the reproduction fidelity of the designed micro-nanostructures is often influenced by experimental writing conditions, including laser power, exposure time, etc. To determine the appropriate writing parameters, in situ characterization of morphological features and surface roughness is needed. Traditional characterization methods for TPP, e.g., scanning electron microscopy and atomic force microscopy, have limited speed and cannot study internal structures without invasive approaches. Optical diffraction tomography (ODT) is an emerging label-free 3D imaging technique based on reconstructing the object's 3D refractive index (RI) distribution with diffraction-limited resolution. Here, we propose a non-invasive solution to fully characterize the TPP-fabricated structures using a high-speed ODT technique, which can eliminate the need for complex sample preparation, such as fluorescence labelling or metal-coating, and achieve a full 3D measurement time within 6 ms. By visualizing and studying different TPP-fabricated structures, including embedded spirals and cubes, via the ODT system, the fabrication quality, including 3D morphological features, exposure levels, and surface roughness, can be examined quantitatively. The results suggest our method can effectively improve the fabrication quality and reproducibility of TPP, generating impact to the nanofabrication community.*

---

## 1. Introduction

As a direct laser writing technique, two-photon polymerization (TPP) has become one of the most widely used manufacturing techniques for the fabrication of 3D micro- and nanostructures [1, 2] in recent years. During the fabrication process, the polymerization is initiated on a photosensitive resin by the nonlinear two-photon absorption effect that only occurs within the focal region of a femtosecond laser [1]. As the properties and functions of a fabricated structure are often influenced by its morphology and refractive index (RI) distribution, characterization is needed to precisely examine the fabricated structure and ensure the result is consistent with the design.

To date, a few methods have been used to characterize TPP-printed structures by offering different resolving capabilities, including scanning electron microscopy (SEM), atomic force microscopy (AFM), focused ion beam sectioning (FIB), x-ray computed tomography (CT), prism coupling method, and laser interferometry. However, these methods have various limitations, e.g., low measurement throughput, high sample invasiveness, sample contact, and small field of view. More importantly, most of the methods cannot visualize the internal structures, but only the surface geometry. Therefore, a fast 3D characterization method that can

simultaneously characterize the surface shape and roughness, internal structures, and RI distribution for arbitrarily-shaped TPP-printed structures is critically needed and has yet to be developed.

Optical diffraction tomography (ODT) has emerged as a powerful tool for label-free 3D characterization of biological specimens [3, 4]. In ODT, the 3D RI distribution of a specimen is reconstructed by measuring the scattered fields coming at different illumination angles, sample rotations, or focal depths. In this work, we present a new method to characterize TPP printed structures based on a high-speed ODT system. The ODT system is integrated with a custom-built DMD-based TPP fabrication system [5] that achieves multi-focus random-access scanning. To evaluate the performance of the ODT-TPP system, we have designed several micro-structures with embedded complex 3D structures via different photoresins (of different RI values). The printed structures are visualized by the high-speed ODT module. The results show that complete 3D morphological information, including internal structures and surface geometry and roughness, of all fabricated structures can be retrieved from the measured 3D RI distributions. For comparison and validation, we used both an SEM and AFM to measure the fabricated structures. The measurements from ODT module are consistent with results from the SEM and AFM. Notably, the ODT module performed

the measurements in only 6 ms and with minimal sample preparation and provided internal structure and 3D RI distribution information that cannot be realized by the SEM and AFM.

## 2. System Design and Results

### 2.1 Setup

Figure 1 presents the design of the ODT-TPP system. The laser source for TPP is an 80 MHz Ti: Sapphire femtosecond (fs) laser (Chameleon Vision S, Coherent) with a central wavelength of 800 nm. First, the laser beam is collimated by lenses L1 and L2 ( $f_1 = 50$  mm,  $f_2 = 50$  mm). Next, a transmission grating G1 (T-1400-800, 1400 lines/mm, Lightsmyth) and a 4-f system (L3 and L4;  $f_3 = 100$  mm,  $f_4 = 250$  mm) are introduced to pre-compensate the angular dispersion induced by the DMD (DMD1, DLP 7000 0.7" XGA, Texas Instruments). After the DMD1 and lens L5 ( $f_5 = 200$  mm), a spatial filter (SF) selects the -1st order diffraction beam in the Fourier plane, which contains the reconstructed wavefronts. Lastly, a 4-f system, i.e., lens L6 ( $f_6 = 54$  mm) and the objective lens (OL1, EC Plan-NEOFLUAR 63 $\times$ , NA = 1.25, Zeiss), relays the scanning laser to the liquid photoresin on a glass substrate, which is affixed to a precision XYZ stage. For the ODT module, a continuous wave (CW) laser beam with a central wavelength of 532 nm is used as the light source (MGL-III-532-300mW, CNI Lasers), which is coupled into a 1 $\times$ 2 single-mode fiber coupler (SMFC). The two output ends of the fiber coupler serve as the sample beam and reference beam, respectively. To ensure uniform sample illumination, the sample beam is collimated by a lens L7 ( $f_7 = 200$  mm) fully fill the aperture of the DMD (DMD2, DLP LightCrafter 9000, Texas Instruments). After DMD2, multiple diffraction orders are generated from the designed binary holograms displayed on DMD2. Next, lens L8 ( $f_8 = 150$  mm) collects the diffraction orders and directs them a third DMD (DMD3, DLP LightCrafter 6500, Texas Instruments), located on the Fourier plane of L8. Notably, here DMD3 functions as a dynamic spatial filter to select the 1st diffraction order (and reject redundant diffraction orders) to enter the subsequent optical system [26]. The filtered beam is reflected by a mirror (M1) and then collimated by a lens L9 ( $f_9 = 200$  mm). Lastly, lens L10 ( $f_{10} = 300$  mm) and the objective lens (OL2, LCI Plan-NEOFLUAR 63 $\times$ , NA = 1.3, Zeiss) form a 4-f system to magnify the angle of the illumination beam over the sample to around 60 degrees. The scattered light from the sample is collected by OL1, which forms an intermediate image at the back focal plane of lens L11 ( $f_{11} = 150$  mm). In the end, the sample beam and the reference beam collimated by lens L12 ( $f_{12} = 150$  mm) are combined through a beam splitter (BS) and relayed to the camera through another 4-f system formed by lens L13 ( $f_{13} = 60$  mm) and L14 ( $f_{14} = 400$  mm). A high-speed camera (Fastcam SA-X2, Photron) is used to record the interferograms at a rate of 8,000 frames per second (fps). From the interferograms, complex sample fields corresponding to different illumination angles are retrieved. Lastly, by using an inverse scattering model based on the first-order Rytov approximation, a 3D RI map of the printed structure can be reconstructed. According to Abbe's diffraction limit, the lateral resolution of our system is

estimated to be around 209 nm [6], while the axial resolution is approximately 2 times or more than the lateral resolution.

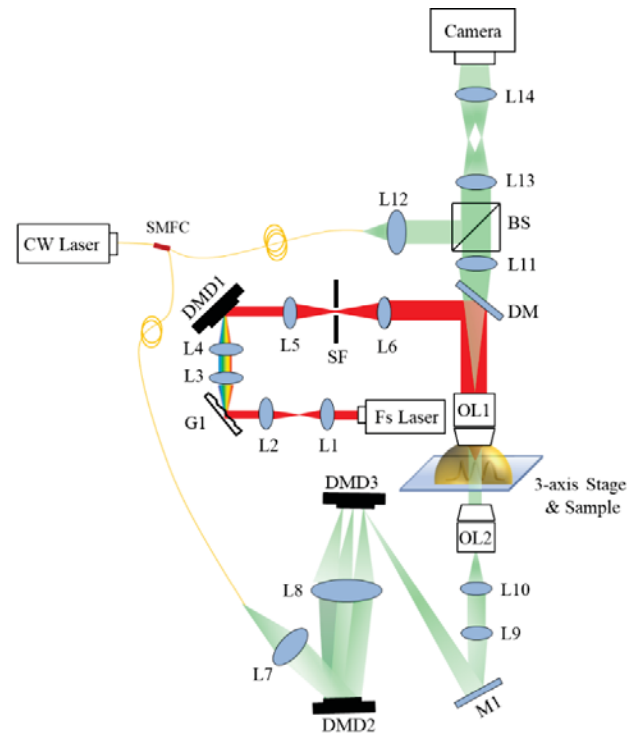


Fig. 1 Design of the integrated ODT-TPP system. L1-L14: lenses; G1: grating; SF: spatial filter; OL1-OL2: objective lens. M1: mirror; BS: beam splitter; and DM: dichroic mirror.

### 2.2.3D Imaging Validation

After the printing and imaging systems are optimized, we designed several 3D micro-structures for subsequent experiments. To validate the 3D morphological structure imaging capability of ODT intuitively, we printed a spiral structure and enclosed it in a shell as designed in Fig. 2(a). The shell size is  $20 \times 18 \times 16.5 \mu\text{m}^3$  with a side wall thickness of  $2.5 \mu\text{m}$ , a top wall thickness of  $6 \mu\text{m}$ , and an open bottom that is attached to a cover glass (No. 1). The enclosed spiral structure has a size of  $10.7 \times 8 \times 8 \mu\text{m}^3$  with a period of  $2.5 \mu\text{m}$ . Using our ODT system, the 3D morphology of the enclosed spiral structure in the shell is fully reconstructed. Figure 3(b) presents the top view of the 3D rendered RI map, while an image stack along the direction, indicated by the black arrow in Fig. 2(a), is shown in Fig. 2(c). From the image stack, the spiral structure is again clearly revealed. For comparison, we also imaged this enclosed spiral under bright-field microscopy. Figure 3(a) and (b) show the bright-field images when the sample is illuminated from the top and the bottom, respectively. As the reflected light by the spiral structure is weak, it cannot be detected in Fig. 3(a). Although the spiral can be detected from the bottom (Fig. 3(b)), the image contrast is poor due to weak light absorption by the spiral structure. To prepare the sample for SEM imaging, we performed sputter coating to make it conductive. Figure 3(c) and (d) show the top and side views from SEM, from which the 3D surfaces are clearly revealed, but the internal structures cannot be observed at all. Note that if the sample was not metal-coated, the SEM images will be blurred (Fig. 3(e) and (f)), especially for the

side-view (Fig. 3 (f)). (The same sample was used for all SEM measurements.) From these studies, we can conclude both the bright-field microscopy and SEM failed to evaluate the fabrication quality of the internal features. In comparison, the ODT system fully revealed the 3D structure with good contrast without complex sample preparation processes.

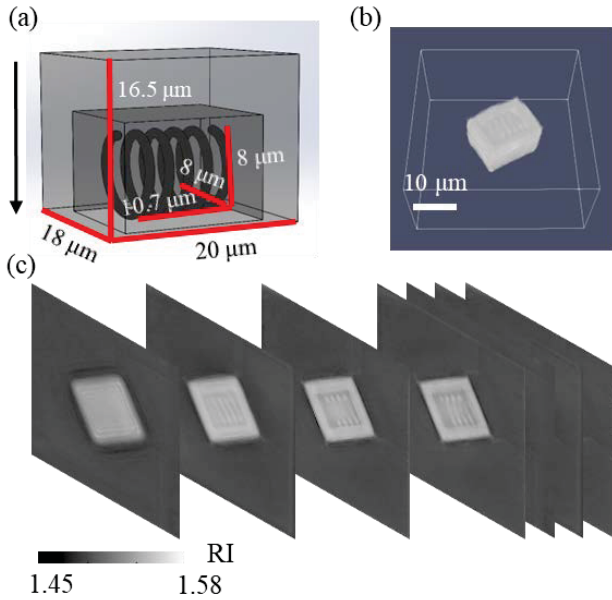


Fig. 2 ODT imaging results of the spiral structure enclosed in a shell.

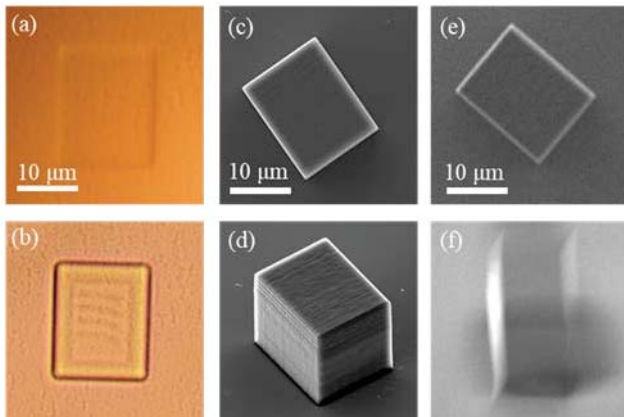


Fig. 3 Bright field light microscopy and SEM imaging results of the enclosed spiral structure in a shell.

### 2.3 Refractive Index Measurement

As the RI distributions of structures fabricated by TPP is essential for designing optical or photonic devices for many applications, such as gradient-index elements, compound lenses for chromatic dispersion controlling, and micro waveguides for photonic integrated circuits [7]. In addition, the RI values of polymerized structures can be influenced by the laser intensity, exposure time, and printing speed [8]. Thus, measuring RI changes will provide insights for us to optimize the laser parameters during the printing of structures.

To test the capability of our system in mapping the RI distributions, we printed three rectangular cuboids with each made

from a unique commercial photoresin material (from Nanoscribe GmbH), following the design in Fig. 4(a), i.e., left (IP-L, RI round 1.518 at wavelength of 532 nm [9]), middle (IP-Dip, RI around 1.553 at wavelength of 532 nm [8, 9]), and right (IP-PDMS, RI around 1.45 at wavelength of 589 nm; note that RI data at 532 nm is not available and we do expect a large difference in RI between 532 nm and 589 nm). Figure 4(b) and (c) are the SEM images at different views. Figure 4(d)-(f) are the corresponding imaging results obtained from the ODT system, from which not only the 3D structural features are obtained, but also the RI values are mapped at all positions. Figure 4(d) presents a bird's eye view of the 3D rendered RI map. The x-y and x-z cross-sections, cut along the yellow and white dotted lines as pointed by the red arrows in Fig. 4(a), are shown in Fig. 4(e) and (f), respectively. After segmentation, we calculated the mean RI values of the IP-L, IP-Dip, and IP-PDMS regions, which are around 1.516, 1.531, and 1.474, respectively. The RI values are consistent with the reported values in Ref. [8, 9], and the small deviations might be due to the fact that the RI of the photoresin may vary with the actual curing conditions [8].

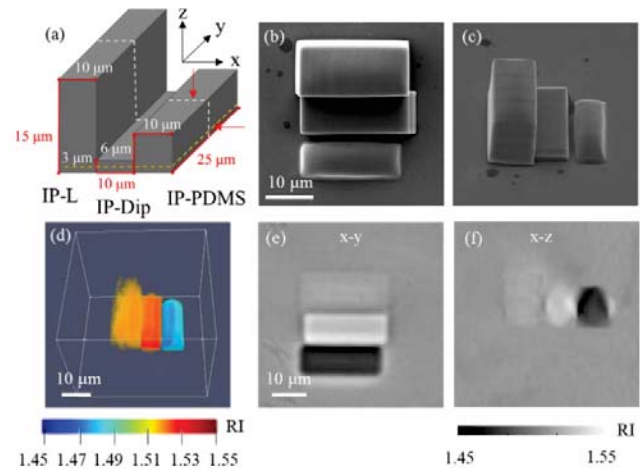


Fig. 4 Refractive index measurements of the rectangular cuboids printed with different photoresins.

### 2.4 Surface Roughness Measurement

Surface roughness is a critical parameter for evaluating the performance of the printed structures for optical applications. For example, the surface roughness of micro-lens needs to be several times smaller than the wavelength of the testing light [10]. Many methods have been proposed for improving the surface roughness of printed structures, such as adaptive stitching and trajectory optimization [11]. However, methods for characterizing the surface roughness of 3D-printed structures are still lacking, especially for high-resolution structures made by TPP.

We printed a cube with a size of  $25 \times 25 \times 7 \mu\text{m}^3$ , following the design shown in Fig. 5(a), and measured its 3D RI map with the ODT system. Using the RI map, we reconstructed the surface profile as shown in Fig. 5(b), while a line profile along the red dotted line is shown in Fig. 5(c). After segmenting the cube height map from the background, we quantified its top surface roughness by calculating the root mean square error, which is found to be around 81.7 nm. To

validate the roughness measurement, we next used the AFM to map the surface profile over the same field of view as the ODT, i.e.,  $56 \times 56 \mu\text{m}^2$ , as shown in Fig. 5(d) - (f). Note that a default low-pass filter was applied in the AFM measurement software, so the curve appears smooth. The surface roughness obtained from AFM is around 81.4 nm, which is consistent with the results from our ODT method.

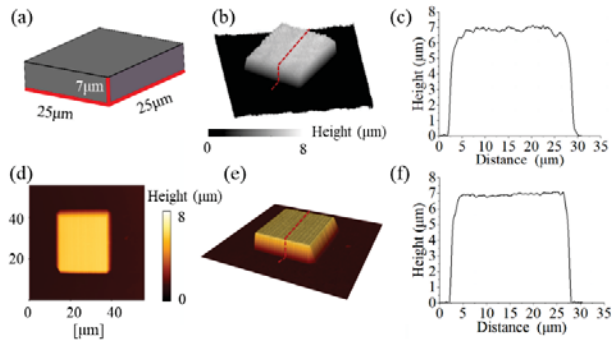


Fig. 5 Top surface roughness measurement of a cube using the ODT system. (a) Isometric view of the cube design.

### 3. Conclusions (Times New Roman 10pt)

In conclusion, we have presented a combined ODT-TPP system that demonstrates high-speed 3D visualization of the internal structures of five different 3D objects at diffraction limited resolution as well as 3D RI mapping. In comparison, conventional characterization methods (i.e., SEM and AFM) have limited measuring capabilities; thus each method or even combinations of these methods cannot fully characterize the feature dimensions, internal structures, and surface roughness of the printed structures. Notably, the ODT measurement is performed in milliseconds, which is more than three orders of magnitude faster than conventional methods. Although the 3D image reconstruction and segmentation time are currently around several minutes, it can be further expedited with parallel computing. We envision our method can be potentially applied for large-scale characterization of micro-nanostructures during the fabrication process and provide feedback for the optimization of the printing parameters in real-time.

### ACKNOWLEDGEMENT

This work was supported by the Innovation and Technology Commission, Innovation and Technology Fund (ITS/178/20FP & ITS/148/20); Research Grants Council, General Research Fund (14209521 & 14209421); and Science, Technology and Innovation Commission of Shenzhen Municipality (STIC) (No. SGDX20201103095001009).

### REFERENCES

1. C. N. LaFratta and T. Baldacchini, "Two-photon polymerization metrology: Characterization methods of mechanisms and microstructures," *Micromachines*, vol. 8, no. 4, p. 101, 2017.
2. H.-B. Sun and S. Kawata, "Two-photon photopolymerization and 3D lithographic microfabrication," *NMR• 3D Analysis• Photopolymerization*, pp. 169-273, 2004.
3. D. Jin, R. Zhou, Z. Yaqoob, and P. T. So, "Tomographic phase microscopy: principles and applications in bioimaging," *JOSA B*, vol. 34, no. 5, pp. B64-B77, 2017.
4. T. Kim et al., "White-light diffraction tomography of unlabelled live cells," *Nat Photonics*, vol. 8, no. 3, pp. 256-263, 2014.
5. Q. Geng, D. Wang, P. Chen, and S.-C. Chen, "Ultrafast multi-focus 3-D nano-fabrication based on two-photon polymerization," *Nat Commun*, vol. 10, no. 1, pp. 1-7, 2019.
6. C. Park, S. Shin, and Y. Park, "Generalized quantification of three-dimensional resolution in optical diffraction tomography using the projection of maximal spatial bandwidths," (in English), *J Opt Soc Am A*, vol. 35, no. 11, pp. 1891-1898, Nov 1 2018, doi: 10.1364/Josaa.35.001891.
7. L. Jonušauskas, T. Baravykas, D. Andriječ, T. Gadišauskas, and V. Purlys, "Stitchless support-free 3D printing of free-form micromechanical structures with feature size on-demand," *Sci Rep-Uk*, vol. 9, no. 1, pp. 1-12, 2019.
8. S. Dottermusch, D. Busko, M. Langenhorst, U. W. Paetzold, and B. S. Richards, "Exposure-dependent refractive index of Nanoscribe IP-Dip photoresist layers," *Opt Lett*, vol. 44, no. 1, pp. 29-32, 2019.
9. T. Gissibl, S. Wagner, J. Sykora, M. Schmid, and H. Giessen, "Refractive index measurements of photo-resists for three-dimensional direct laser writing," *Optical Materials Express*, vol. 7, no. 7, pp. 2293-2298, 2017.
10. R. Guo, S. Xiao, X. Zhai, J. Li, A. Xia, and W. Huang, "Micro lens fabrication by means of femtosecond two photon photopolymerization," *Opt Express*, vol. 14, no. 2, pp. 810-816, 2006.
11. C. R. Ocier et al., "Direct laser writing of volumetric gradient index lenses and waveguides," *Light: Science & Applications*, vol. 9, no. 1, pp. 1-14, 2020.